Challenges in electron cyclotron resonance plasma etching of LiNbO₃ Surface for fabrication of ridge optical waveguides

Naoki Mitsugi and Hirotoshi Nagata [a)]
Optoelectronics Research Division, New Technology Research Laboratories,
Sumitomo Osaka Cement Co., Ltd., 585 Toyotomi-cho, Funabashi, Chiba 274-8601, Japan

Kaori Shima and Masumi Tamai
Advanced Material Research Division, New Technology Research Laboratories,
Sumitomo Osaka Cement Co., Ltd., 585 Toyotomi-cho, Funabashi, Chiba 274-8601, Japan

Ridge-shaped optical waveguide are promising structures to provide broadband characteristics for LiNbO₃ (LN) base optoelectronic devices. In this regard, electron cyclotron resonance plasma etching with fluorocarbons have been commonly applied in the preparation of ridge waveguides, 3-5 µm in height, but certain fabrication problems need investigation and clarification. The etched LN surface was found to be covered with LiF leading to a weak adhesive strength for the overlayer, such as a SiO₂ film, over the ridge waveguides. When CF₄ etchant was used, a notch appeared along the foot of the ridge waveguides. The notch was a possible origin for the chipping of the waveguides. Such an undesirable notch was found to be prevented by the use of a CHF₃ etchant. Here, these inevitable problems during the plasma etching of the LN were presented and discussed. © 1998 American Vacuum Society. [S0734-2101 (98) 11204-6]

. INTRODUCTION

LiNbO₃ (LN) based optical waveguide devices are commonly used in optical fiber communication systems as an external optical intensity modulator and an optical polarization scrambler. Current LN devices are designed to be operated at 2.5-5 Gb / s speed, and the fabrication technology for them is simple. Over the z-cut LN substrates with Ti-indiffused waveguides, an approximately 1 ∝m thick SiO₂ buffer layer, a thin Si layer, and approximately 15 ∝m thick gold electrodes are formed using a conventional film deposition technology. By increasing the thickness of the buffer layer and the electrodes, the operation speed of the device can be increased. However, in order to realize a LN modulator faster than 40 Gb /s, the distribution of the electric field applied to the device must be adjusted to concentrate on the waveguides by machining the LN surface. Fabrication of ridge shaped waveguides is an example of such technology and recently, Noguchi et al. reported 100 Gb / s LN modulators with 3-4 ∝m high ridge waveguides. [1-3]

As a method for fabrication ridge waveguides, both wet and dry etching techniques have previously been demonstrated. Wet etching was performed on the +z face of the LN substrates using a HF / HNO₃ mixture following a proton-exchange treatment of the substrate surface.[4,5] This method was reported to produce a smooth etched surface compared with dry etching. However, use of the +z face is not favorable for the preparation of conventional Ti-indiffused waveguides because of the occurrence of domain inversion during the thermal diffusion process of Ti.[6,7] The alternative dry etching can be applied irrespective of the substrate orientation. Chemically assisted etching with fluorocarbon

Plasma, such as an electron cyclotron resonance (ECR) Plasma etching, is frequently used for preparation of ridge Waveguides. Actually, the ECR etching process has been apPlied to achieve ultrahigh speed LN modulators.[1-3] HowEver, a problem in the dry etching process of the LN substrates has not clarified yet. Generation of Lif precipotates on the etched surface. as recently reported by us, may have been the cause of the problem in the device fabrication processes.[8,9] The purpose of this article is to investigate and clarify such problems occurring in the fabrication of high speed LN modulators with ridge waveguide. A possible solution can be proposed for some of these problems. For instance, when the SiO₂ buffer layer was formed on the etched LN surface, the adhesive strength of the film decreased and the layer peeled off during the substrate cutting process. Such weak adhesive strength was considered to come from the existence of a LiF layer on the LN surface, which was induced by ECR etching with fluorocarbons. The second problem was a chipping of the ridge waveguides and the reason for this phenomenon is discussed.

. EXPERIMENTAL PROCEDURES

The dry etching of the LN substrates was carried out using a commercial ECR etcher, ANELVA model L-310R, with CF₄ or CHF₃ as an etching gas. A -z-cut LN wafer having a 3 in. diam and a 0.5mm thickness was placed on a silicon carbide substrate holder which faced the plasma chamber The distance between the substrate and the acceleration electrode at the plasma outlet was about 20cm. After the etching chamber was evacuated to under 4× 10⁻⁴ Pa, the etching gas was introduced at a rate of 3 sccm and the pressure was kept at about 4 × 10⁻² Pa. The electric power supplied to the microwave generator was 400W, and the magnet voltage and the ion acceleration voltage were set to 80 and

---

(a)

Distance Between Electrodes : 25μm
Etching Width
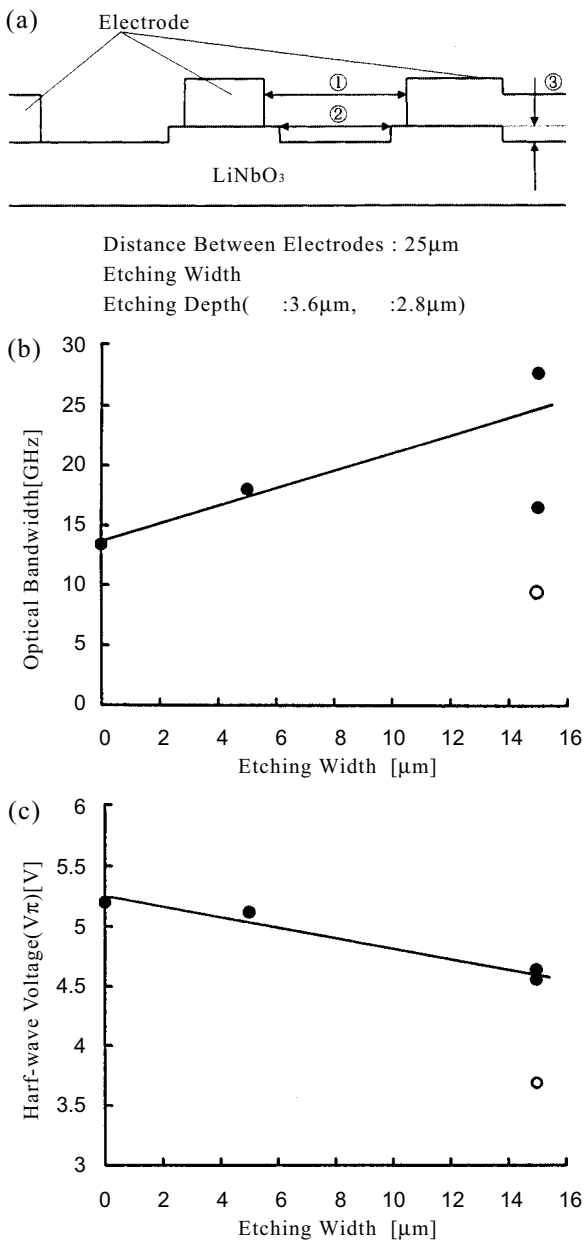Etching Depth(:3.6μm,   :2.8μm)

(b)

(c)

FiG. 1 (a) Schematic illustration of cross section of the fabricated LN MZ optical intensity modulator having ridge waveguides. (b) Optical bandwidth and (c) halfwave voltage V   measured for the fabricated devices as a function of the gap distance between the ridge MZ waveguide arms.

500 V, respectively. During the etching, the substrate holder was water-cooled at 21 ºC and rotated (17 rpm). Under these etching conditions, typical etching rates of 800 nm / h by CF_4 and 700 nm / h by CHF3 were obtained for the LN. The deviation in etched depth for a 3 in. diam substrate was ± 20 nm for 240 nm deep etching by CHF_3, for instance.

Patterned etching of the LN for fabrication of ridge waveguides was performed using a Ni film mask. A conventional resin mask could not endure the several-hours-long etching for 3-5 μm depth. The etching rate ratio of the LN to the Ni film was measured at about 3.7 independent of the etching gas. The Ni film mask was prepared on the LN substrate by conventional photolithography and a lift-off process

using vacuum evaporation deposited 1.2μm thick Ni film. Recently, an electroplated Ni film was tested as an etching mask and found to be just as suitable as the thicker mask. After ECR etching, the remaining Ni was easily removed using dilute HNO_3 at room temperature.

Inspection of the etched substrates was performed using a secondary electron microscope (SEM: JEOL model JSM T-330A) and an atomic force microscope (AFM: Seiko Instrumentals SPI-3700). The etched depth and surface profile were measured by a stylus method using a probe with 1.25 μm diam (DekTak). Chemical analyses of the surface were done with an Auger electron spectrometer (AES:JEOL model JAMP-10SX) and an electron probe microanalyzer (JEOL model JXA 8800).

. RESULTS AND DISCUSSION

A. Formation of rldge waveguides

Figure 1(a) shows a schematic illustration of the ridge waveguides fabricated on the z-cut LN substrate. After the Mach-Zehnder (MZ) type waveguides were formed on the substrate by a conventional Ti-indiffusion technique, the rectangular spaces on both side of the MZ waveguide arms were etched to 2 8 ∞m in depth, 40mm in length along the waveguide and 5 or 15∞m in width. The etched width corresponded to the gap between the obtained ridge waveguides in Fig. 1(a). Then, the SiO_2 buffer layer was deposited by rf sputtering from a SiO_2 target with an Ar / O_2 mixture to a thickness of 1.2 ∞m, and a 100nm thick Si layer was sputter deposited [not shown in Fig. l(a)]. Over the ridge waveguides covered by the SiO_2 and Si layers, 17∞m thick coplanar gold electrodes were formed by electroplating to give a 25 ∞m gap between the hot and ground electrodes.

The effects of the ridge waveguides on device characteristics are shown in Figs. 1(b) and 1(c) for the optical bandwidth and the drive voltage V   , respectively. Increasing the gap between the MZ waveguide arms, expanded the optical bandwidth and V   was reduced. Results indicated the application of ridge waveguides was effective in realizing broader band LN waveguide modulators. However, in the fabrication
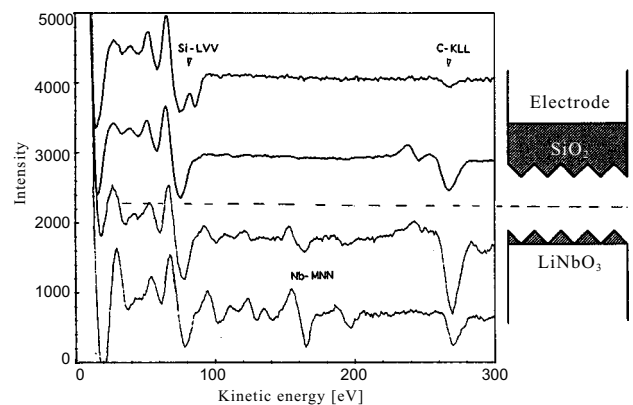

Fig. 2.   Result of AES analyses for the failed device, in which the surface electrodes and the SiO_2 buffer layer peeled off from the etched LN wafer surface.

process of LN ridge waveguides, problems emerged which needed to be solved for improvement of the device fabrication yield.

B. Chemical deterioration of etched surface

In the fabrication of LN modulators with ridge waveguides, some of the modulators failed because of a peeling off of the thick ground electrodes during the cutting process of the LN chips from the wafer. The ground electrodes were formed over the ECR etched LN surface via. the SiO_2 buffer layer. In our experience on thousands of conventional LN modulators made without the ECR etching process, such failure has rarely been observed. Figure 2 shows the AES profiles for surfaces of the peeled electrode and the substrate. The dashed line in the figure denotes the peeled position, and the profiles over and under the dashed line denote the peeled electrode underneath and the remaining substrate surface, respectively. The other two profiles were measured after a few minutes of Ar ion etching of the corresponding surfaces to exclude the effect of surface contamination. As is seen, the Auger electron peaks come from Nb were detected only from the substrate, indicating that the electrode peeled off at the
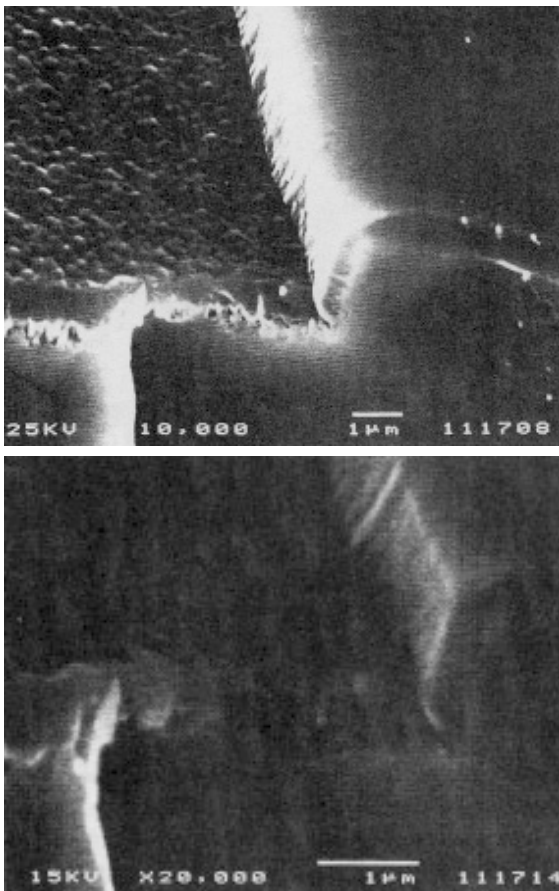

Fig. 3.   SEM image of the cross-section of the LN wafer with ridge waveguides and the buffer layer. The ridge waveguides were prepared by ECR etching using CF_4
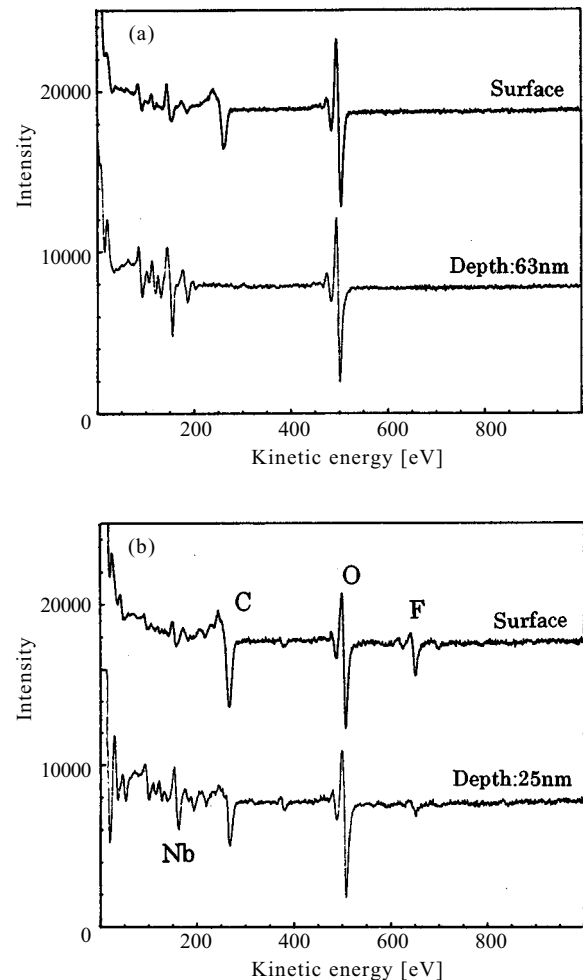

Fig. 4.   AES measurement results for (a) virgin LN surface and for (b) the ECR etched surface with CF_4

boundary of the LN and the SiO_2 buffer layer. In other words, the adhesive strength between the ECR etched LN and the SiO_2 was weak.

Figure 3 shows a SEM image of a cross section of the ridge waveguide with only the 1.2 μm thick SiO_2 buffer layer without the electrodes. The boundary between the buffer layer and the LN ridge waveguide was smooth and the buffer layer and waveguides adhered closely to each together. However, the boundary on the etched LN surface was rough accompanied with small voids, suggesting the inferior adhesion of the buffer layer.

Results of the AES examination of the ECR etched surface, as shown in Figs. 4(a) for the virgin LN surface and 4(b) for the etched surface, show significant amounts of fluorine and carbon from the ECR etched surface. These contaminants are thought to deteriorate the adhesive strength of the buffer layer on the etched LN surface. The origin for the extrinsic contaminants was previously investigated and found to be precipitation of LiF and polymers, possibly due to the etching gases (CHF_3 and CF_4).[8,9] In particular, the LiF precipitates were found to be crystalline in the CF_4 etching, while amorphous in the CHF_3 etching.[9] Presumably, the ex-
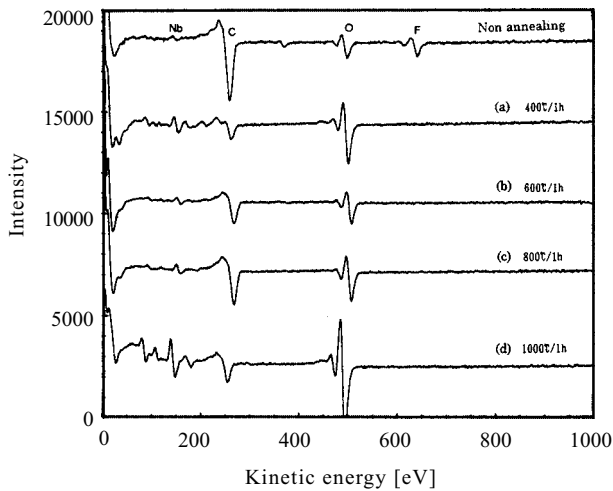
FIG. 5 AES analysis results for the LN surface etched by CHF₃ ECR plasma measured before (top of the figure) and after the annealing in O_2 (a) at 400 ºC, (b) at 600 ºC (c) at 800 ºC, and (d) at 1000 ºC

Fig. 6. AFM images for the LN surface etched by CHF₃ ECR plasma observed after the annealing in O_2 (a) at 400 ºC, (b) at 600 ºC, (c) at 800 ºC, and (d) at 1000 ºC.

istence of such plasma species as HF in the ECR plasma affects the structure of the deposits.

In order to improve buffer layer adhesion, a method to remove surface contaminants was investigated. The LiF precipitates at least, they were easily removed by wet etching the substrate in dilute HNO_3 at room temperature. Alternatively, a postannealing of the substrate in an oxidizing atmosphere was found to be effective in excluding the LiF and reducing the carbon contaminants. For instance after 3 h of etching using CHF₃, the samples were placed in a platinum box and annealed for 1 h in flowing O_2. Figures 5(a)-5(d) show the AES results for samples annealed at 400 ºC in (a), 600 ºC in (b), 800 ºC in (c) and 1000 ºC in (d). With the 400 ºC annealing, the LiF precipitates seemed to be completely removed, judging from the absence of the F peak in the AES profile. Further, the intensity of the C peak decreased with increasing annealing temperature, and the Nb peaks appeared in the AES profiles.

Figures 6(a)-6(d) show AFM images corresponding to the samples shown in Figs. 5(a)-5(d). The surface morphology changed significantly, depending on the annealing temperatures. The peak-to-peak surface roughness measured for the 5μm× 5 μm area was (a) 13.6 nm, (b) 22.7 nm, (c) 41.5 nm and (d) 4.5 nm, while 16.6 nm for the as-etched surface. Although the surface contaminants due to the etching could be largely reduced, the morphology was not improved by the postannealing.

The ridge waveguide devices were prepared again, adopting processes for removing the etching deposits (especially the LiF) before the buffer layer deposition process. The above described O_2 annealing at 600 ºC and the alternative HNO_3 etching were attempted, and no buffer layer or electrodes peeled off, even after machining the wafer. The adhesive strength of the buffer layer was improved by removing the etching deposits on the LN surface.
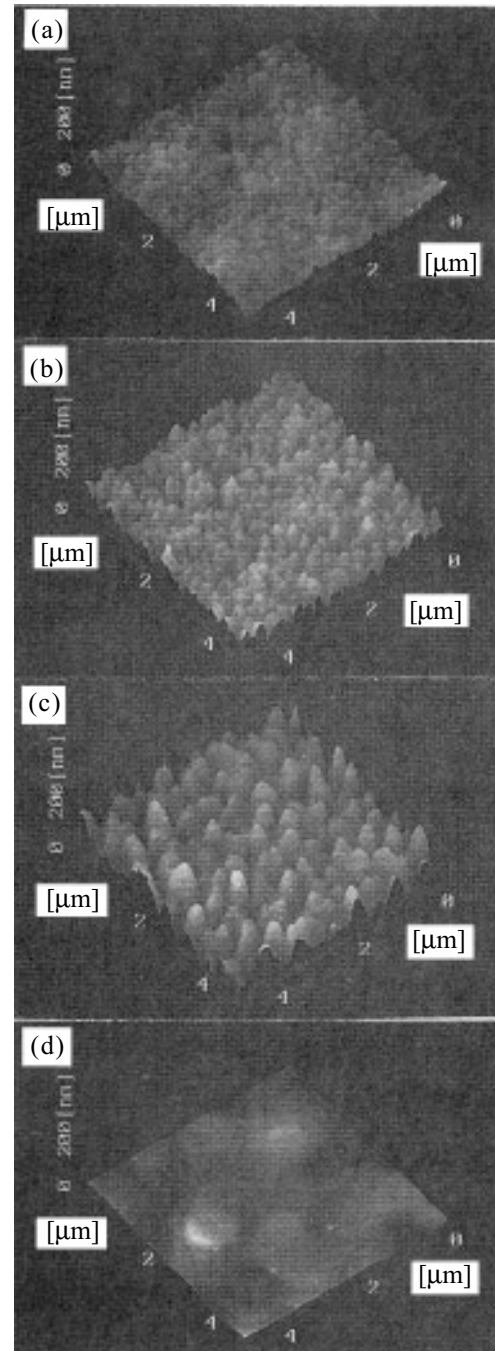
C. Mechanical problems in etched surfaces

In addition to the chemical problems, a catastrophic mechanical problem occurred in the fabrication of the ridge waveguide devices. Figure 7 shows the SEM image for the mechanically broken ridges, in which the waveguide was also broken and could not transfer any optical signal. Such failure was found frequently after the buffer layer deposition on the substrates ECR etched by CF₄. With increasing the buffer layer thickness, the number of broken waveguides in-
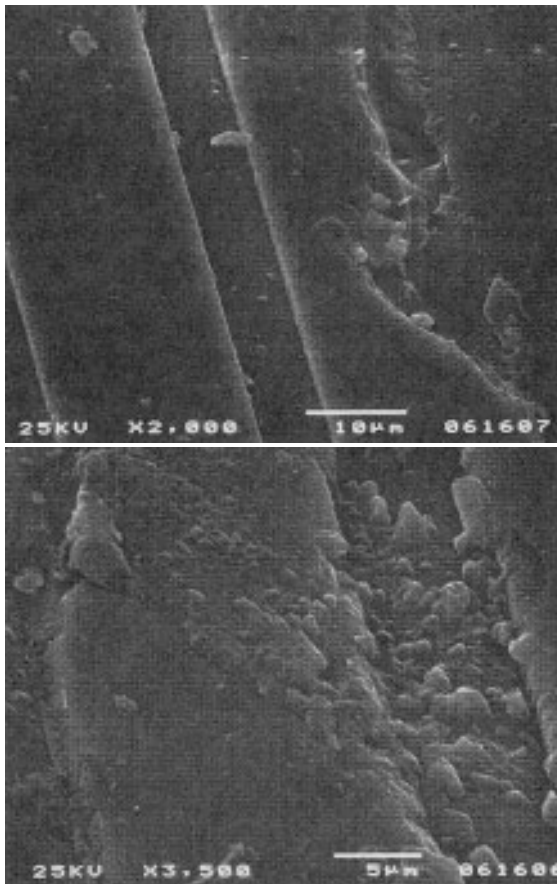
FIG. 7.   SEM images of the broken ridge waveguides after the Si0₂ Buffer layer deposition process.
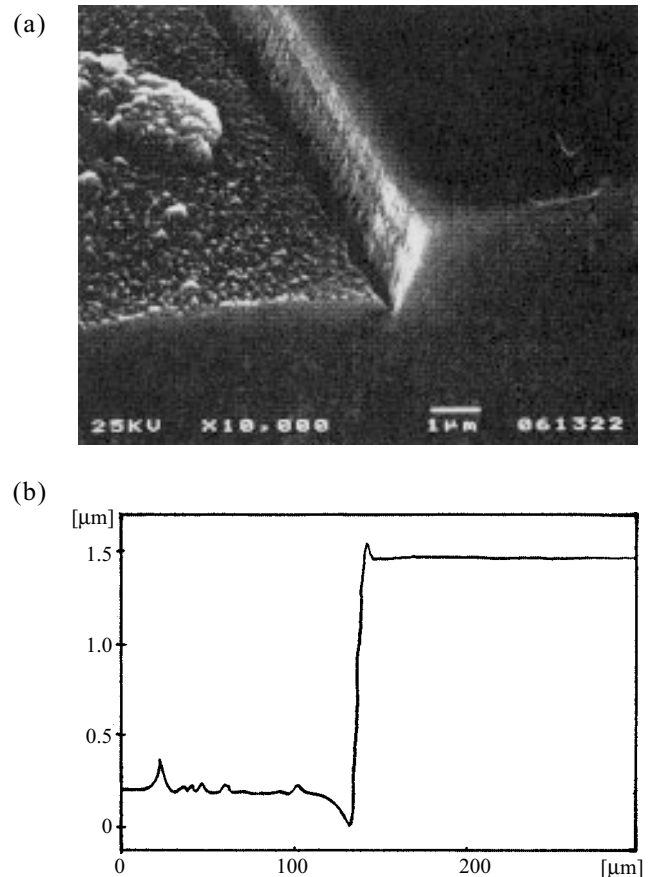
FIG. 8.   (a) Cross-sectional SEM image of the ridge waveguide prepared by the CF₄ ECR plasma etching, and (b) the corresponding surface profile measured by the stylus method.

creased and the fabrication yield for the devices deteriorated significantly (almost all device chips in the wafer failed due to the brake at somewhere in the waveguides).

As a reason for the damaged ridge waveguides, surface stress due to the buffer layer formation was considered. Internal stress of the sputtering-deposited SiO_2 buffer layer on the LN was previously found to be compressive stress and tensile stress for the LN surface. On the other hand, growth of a notch line along the ridge waveguides, as shown in Fig. 8, was found for the samples ECR etched by CF_4. The SEM image of Fig. 8(a) was observed before the buffer layer deposition. There was a possibility that the notches were the origin of the fractured ridge waveguides with the tensile stress on the LN surface being induced by the buffer layer deposition.

For instance, the magnitude of the surface stress was calculated from a wafer deflection measured for a sample with a l.2 μm thick sputtering deposited SiO_2 buffer layer. The wafer deflection was measured by a stylus method for a 50 mm distance along the wafer diameter. The change of the wafer deflections before and after the buffer layer deposition was $+ 16 \mu m$ per 50mm. The resulting tensile stress was estimated to be $1.7\text{-}4.5 \times 10^8$ N/m₂ using a Young's modulus for the LN of 7-7.5 Pa, a Poisson ratio of 0.2-0.5 and a wafer thickness of 0.5mm This stress was comparable with

the strength measured for the LN crystal, suggesting the ridge breaks were due to the buffer layer deposition. Here, the strength of the LN crystal was measured by a four-point bending method to be approximately 2×10^8N/m² (the 63.2% characteristics strength in the Weibull plotting of the results for 24 test pieces). Because the broadband LN devices commonly demand thicker and dense SiO_2 buffer layers, efforts to reduce the film internal stresses are needed and are being investigated.

Another concern with the ridge waveguide fabrication was notches along the ridge waveguide foot formed during the dry etching (see Fig. 8). This problem was found to be improved by changing the etching gas from CF_4 to CHF_3, although the reason for the improvement is not known at this time. Figures 9(a) and 9(b) show the SEM image and the surface profiles, respectively, of the ECR etched ridge waveguides using CHF_3. The ridges with 4-5μm height were successfully fabricated over the 3 in. diam LN wafer without any notches. It was found that size and crystalline structure of the surface precipitates differed depending on the etching gas; large particles consisting of crystalline LiF for the CF_4 etching, while small particles consisting of amorphous LiF for the CHF_3 etching.[9] Further, in the case of CF_4 etching, the boundary between the surface precipitates and
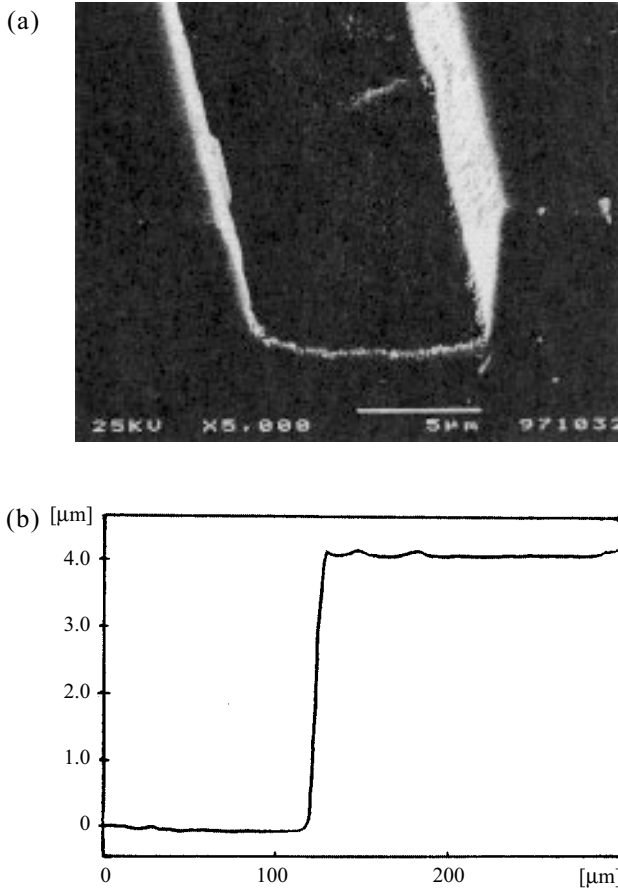
(a)

(b) [μm]

FIG. 9. (a) Cross-sectional SEM image of the ridge waveguide prepared by the CHF₃ ECR plasma etching, and (b) the corresponding surface profile measured by the stylus method.
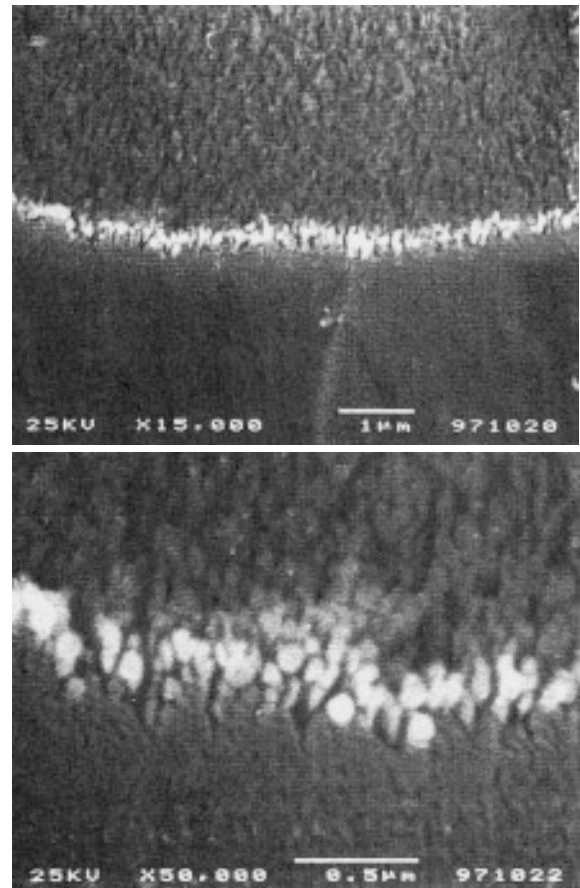
FIG. 10. Cross-sectional SEM image of the ridge waveguide prepared by the CF₄ ECR plasma etching.

the LN wafer was also found to be roughened as shown in Fig. 10. Even after the removal of the surface precipitates by the methods described in the previous section, the notches did not disappear and the rough LN surface appeared. Such difference in the surface reaction depending on the etching gas was considered to be one of the reasons for the improvement of etched surface morphology by using CHF₃ instead of CF4.

Some of the ridge waveguide devices were fabricated using a CHF₃ etching process, but without any improvement concerning the buffer layer deposition process; e.g., the devices of Fig. 1. Although the problem of the buffer layer stress was not eliminated, the breaks in the ridge waveguides could be largely suppressed and the fabrication yield increased.

D. Other problems due to plasma processing

In the plasma process for LN wafers such as the dry etching described here and the sputtering film deposition process,
generation of pin holes through the wafer was observed although it was not common. In our experience, such failure was found once or twice per several times of the ECR etching process.
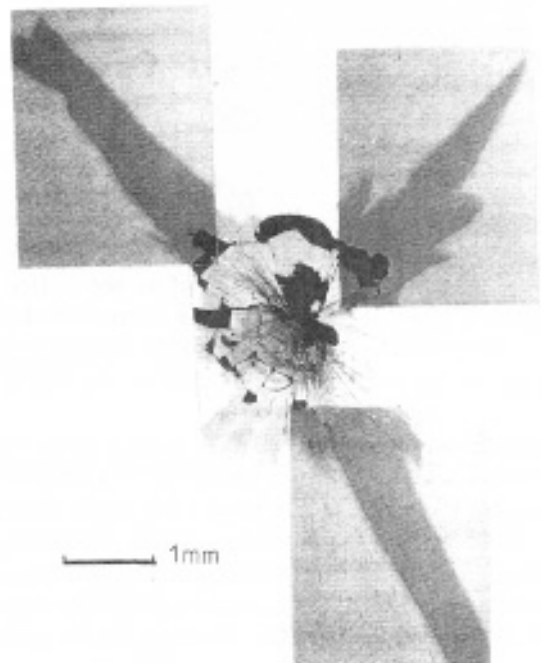

FIG. 11. Example of the pin hole observed at the center of the LN wafer after ECR etching process.

Figure 11 shows an example of a pin hole of approxi- Mately 40μm size which was found almost at the center of the 0.5mm thick z-cut wafer after the etching. During the plasma process, a plasma spark occurred sometimes on the wafer surfer possibly due to pyroelectrically induced charges on the LN surface as a result of temperature increase of the surface by the process. Such charges generated largely for the z-cut LN surface because of the pyroelectric effect along the crystal z axis. At this moment, we consider that the observed pin hole were caused by dielectric breakdown of the material due to the plasma spike. One reason for this speculation is that such failure was not observed in the simi- lar process for x-cut LN wafers, in which surface an occur- rence of the pyroelectric effect can be neglected.

. CONCLUSION

Problems in the fabrication of LN ridge waveguide de- vices were observed. Weakening of over-layer adhesion strength and ridge waveguide mechanical strength were found to be the cause of reduced fabrication yield. These phenomena were found to come mainly from the chemical deterioration of the ECR etched LN surface and to be im- proved by changing the process conditions. Both in situ (choice of the etching gas, etc.) and *ex situ* (postannealing, etc.) methods were effective in reducing the failure. Present experiments indicated that CHF_3 is superior to CF_4 for ECR dry etching of LN wafers due to suppressed deterioration of the surface.

[1] K. Noguchi, O. Mitomi, H. Miyazawa, and S. Seki, J. Lightwave Tech- nol. **13**, 1164 (1195).

[2] K. Noguchi, O. Mitomi, K. Miyazawa, *Optical Fiber Communica- tion, OFC'96 Technical Digest* (Optical Society of America, Washington D.C., 1996), p. 205.

[3] K. Noguchi, O. Mitomi, K. Kawano, and M. Yanagibashi, IEEE Photon- ics Technol. Lett. **5**, 52 (1993)

[4] F. Lanrell, J. Webjorn, G. Arvidsson, and J. Holmberg, J. Lightwave Technol. **10**, 606 (1992).

[5] R. S. Cheng, W. L. Chen, and W. S. Wang, IEEE Photonics Technol. Lett. 7, 1282 (1995).

[6] S. Miyazawa, J. Appl. Phys. **50**, 4599 (1979).

[7] C. Q. Xu, H. Okayama, and M. Kawahara, Appl. Phys. Lett. **64**, 2504 (1994).

[8] K. Shima, N. Mitsugi, and H. Nagata, J. Mater. Res. **13** 527 (1998).

[9] H. Nagata, N. Mitsugi, K. Shima, M. Tamai, and E. M. Haga, J. Cryst. Growth (to be published).